

MODELING AND ANALYSIS OF HELICOPTER ROTOR INSTABILITIES USING SYMBOLIC PROCESSING AND CONTROL SYSTEM DYNAMICS SOFTWARE

C. S. Robinson, E. R. Wood and R. L. King

Naval Postgraduate School
Monterey, California U.S.A.

I. INTRODUCTION

Current trends in helicopter technology and manufacturing have favored the use of bearingless rotor designs that make use of advanced composite materials. These designs offer many advantages over more conventional articulated rotors when reliability and maintainability are considered. Additionally, future helicopter development promises the inclusion of smart material technology and active rotor control as engineers strive to optimize helicopter vibrational, acoustical, and aeromechanical characteristics. A potential payoff from the successful use of the technologies mentioned above is the damperless rotor; a design that offers major returns in the form of decreased rotor system weight, reduced parts count, and reduced maintenance requirements. The goal of the study was to develop a flexible computational tool to analyze the dynamic and aeromechanical behavior of advanced technology coupled rotor/fuselage systems. A series of programs were developed utilizing the symbolic processing software, MAPLE®, the computational software, MATLAB®, and the dynamic simulation software, SIMULINK®. It was desired that the computational tool be simple to understand and lend itself to easy reprogramming by any user knowledgeable in the field of dynamics and in the use of the software packages noted above. It was also desired that the developed programs allow for a reasonable degree of sophistication so that the effects of introducing advanced technologies into rotor system designs could be accurately modeled.

II. THE COMPUTATIONAL TOOL

The computational tool is comprised of three basic parts:

1. Derivation and formatting of the equations of motion by symbolic manipulation.
2. Automatic generation of computer code from the algebraic representation of the equations of motion.
3. Incorporation of the generated computer code into a control system/simulation environment.

The initial work focused on modeling the phenomenon of ground resonance. A helicopter was modeled using spring restrained rigid rotor blades attached to a spring mounted rigid fuselage. Two cases were explored. The first case was a simple model, similar to that used by Coleman and Feingold [Ref. 1]. This case allowed for rotor blade lead-lag and fuselage translational degrees of freedom and was absent of aerodynamic effects. The second model was more complex, with fuselage rotational degrees of freedom, rotor blade flap, and aerodynamic effects.

The first part of the process was accomplished using the symbolic processing software MAPLE® to systematically apply Lagrange's equation (Eqn. (1)) ,

$$\frac{d}{dt} \left(\frac{\partial T}{\partial \dot{q}_i} \right) - \frac{\partial T}{\partial q_i} + \frac{\partial U}{\partial q_i} + \frac{\partial D}{\partial \dot{q}_i} = Q_i \quad (1)$$

where, t = time, q_i = generalized displacement, Q_i = generalized force, T = system kinetic energy in terms of system degrees of freedom, U = system potential energy, and D = system dissipation.

The symbolic program starts off by deriving expressions for rotor blade kinetic energy in terms of system degrees of freedom. The program automatically applies the necessary coordinate transformations so that the velocity of an arbitrary point on a rotor blade elastic axis is expressed in inertial coordinates.

The expressions for fuselage kinetic, potential and dissipative energy as well as the

expressions for rotor blade potential and dissipative energy are entered into the symbolic worksheet directly by the user. For example, the fuselage kinetic energy due to fuselage translational motion can be entered as

$$(T_F)_{trans} = \frac{1}{2} M_1 \dot{u}_1^2 + \frac{1}{2} M_2 \dot{u}_2^2 \quad (2)$$

and the k^{th} rotor blade potential energy due to rotor blade flapping and lagging motion can be expressed as

$$(U_B)_k = \frac{1}{2} K_\beta \beta_k^2 + \frac{1}{2} K_\zeta \zeta_k^2 \quad (3)$$

where M_1 = effective mass of fuselage in x-direction, M_2 = effective mass of fuselage in y-direction, u_1 = fuselage displacement in x-direction, u_2 = fuselage displacement in y-direction, K_β = lumped effective rotor blade/flexbeam stiffness in the flap direction, K_ζ = lumped effective rotor blade/flexbeam stiffness in the lead-lag direction, β_k = the flap displacement of the k^{th} rotor blade, and ζ_k = the lead-lag displacement of the k^{th} rotor blade.

With the energy expressions defined for each component of the rotor/fuselage model, the contributions are added and processed in a Lagrangian derivation by the symbolic processing program. The result is a system of second order nonlinear differential equations stored symbolically in a vector of the following form

$$\bar{F}(\ddot{\vec{x}}, \dot{\vec{x}}, \vec{x}, t) = 0 \quad (4)$$

These results are further rearranged into the form shown in Eqn. (5).

$$[A(\dot{\vec{x}}, \vec{x}, t)] \ddot{\vec{x}} = \bar{f}(\dot{\vec{x}}, \vec{x}, t) \quad (5)$$

Here, A is an $n \times n$ (n is the number of system degrees of freedom) matrix of coefficients of the second derivative terms, \bar{f} is a vector containing the system elastic, dissipative, generalized force and nonlinear terms, and \vec{x} is the vector of degrees of freedom.

At this point the MAPLE[®] program performs the second part of the process that makes up

our computational tool. The algebraic expressions in the matrix, A , and vector, \bar{f} , are automatically converted to optimized (coded so that a processor performs the minimum number of floating point operations required to evaluate the elements of A and \bar{f}) C or Fortran code.

The third part of the process is completed when the generated code is incorporated into the MATLAB[®]-SIMULINK[®] environment via the S-function interface. An S-function is a generically formatted subroutine which communicates the dynamics of a system to a numerical integration routine so that those dynamics can be simulated and/or incorporated into more complex models in a straight forward manner. An S-function can be coded in either C, Fortran, or MATLAB[®] m-file format.

The equations of motion are numerically integrated in their complete nonlinear form using the following format,

$$\begin{aligned} \dot{\vec{x}} &= \vec{w} \\ \dot{\vec{w}} &= [A]^{-1} \bar{f} \end{aligned} \quad (6)$$

Eqn. (6) is the first order representation of Eqn. (5). Eqn. (6) is used to evaluate the system state derivatives at each major and intermediate time step (depending on which algorithm is selected). These state derivatives are then used by a numerical integration algorithm included with the SIMULINK[®] software package (Runge-Kutta 4-5 primarily used for this study). For a complete discussion of the development of the computational tool and SIMULINK[®] S-functions, see Refs. 2 and 3.

III. SIMULATION RESULTS

This section displays results of several simulations and demonstrates the unique capabilities and flexibility of this new nonlinear modeling method. Direct simulation allows analysis of any number of different configurations or scenarios, such as non-isotropic hub, one damper inoperative, or even simulated rotor blade damage. Though the time history plots in the following subsections do not indicate it, SIMULINK[®] offers the useful capability of being able to visualize the dynamics of a model as they progress, which can add valuable insight into the phenomenon being studied.

The basic case is an articulated 3-bladed rotor which is intentionally set up with zero damping and with a rotor speed set approximately at the center of the regressing lead-lag mode instability region. The first set of simulations will demonstrate the system behavior when excited with an initial fuselage velocity. Figure 12.1 and Figure 12.2 show the lead-lag time histories and the fuselage center of mass trajectory (displacements are in feet) for the basic case.

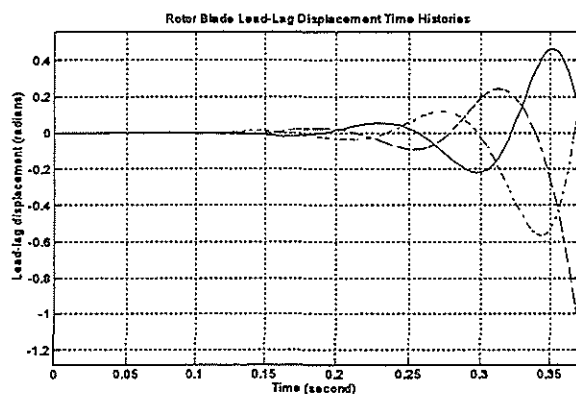


Figure 12.1 Rotor Lead-lag Displacements for Basic Parameter Case Settings, Center of Self Excited Region.

As expected, Figures 12.1 and 12.2 show the rapid divergence of the model as a result of being in the center of the self excited region. The diverging spiral path of the fuselage center of mass is a characteristic result of the regressing lead-lag mode instability.

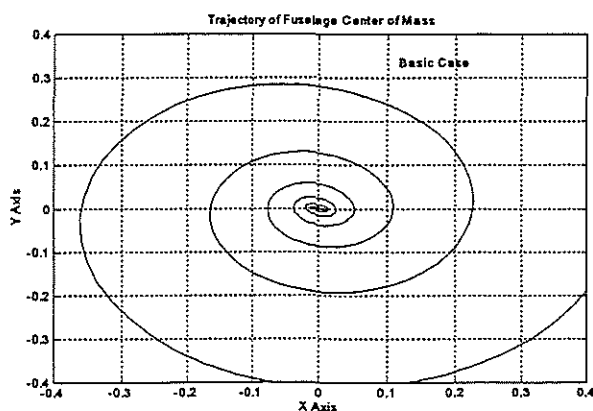


Figure 12.2 Fuselage Trajectory for Basic Parameter Settings, Center of Self Excited Region.

Figures 12.3 and 12.4 show the corresponding results for operation below the

self excited region. Figure 12.3 shows a beat or modulation of the blade response but no divergence. The beat phenomenon indicates the blade lead-lag motion consists of two dominant modes closely spaced in frequency. The fuselage center of mass trajectory shown in Figure 12.4 shows an elliptical path with the major axis of the ellipse rotating about the zero displacement position. Both the beat phenomenon and the precession type motion of the hub are characteristic behavior of a system operating outside the self excited region. It is interesting to point out that this behavior is also characteristic of spherical pendulums.

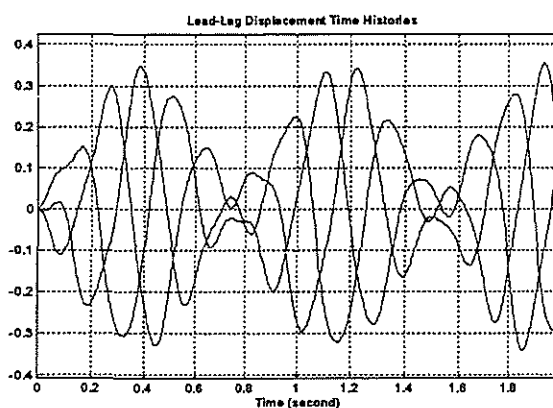


Figure 12.3 Rotor Lead-lag Time Histories, Rotor Speed Below Self Excited Region

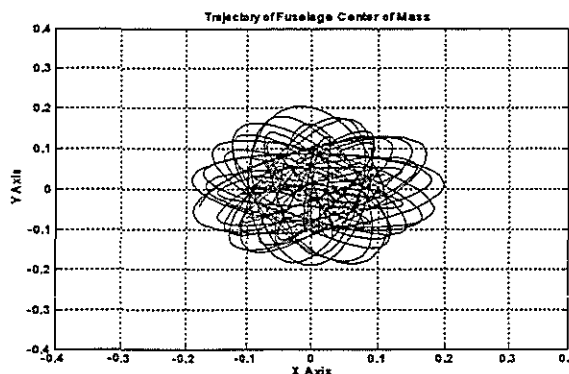


Figure 12.4 Fuselage Trajectory for Basic Parameter Settings, Rotor Speed Below Self Excited Region

Figures 12.5 and 12.6 show the results of a simulation where rotor speed was set above the self excited region. Again, the fuselage exhibits an elliptic whirling motion with the major axis of the ellipse rotating about the zero displacement position while the blade lead lag motion follows a beat pattern.

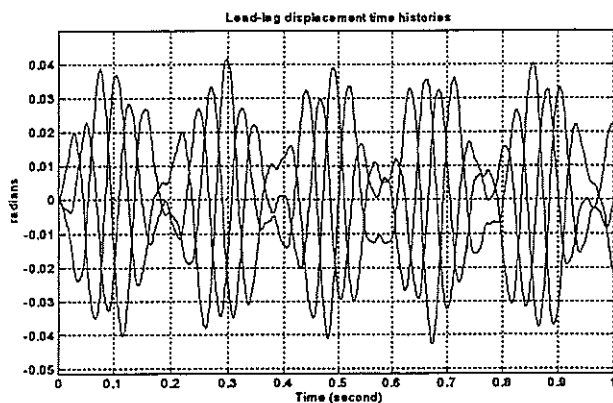


Figure 12.5 Rotor Lead-lag Time Histories, Rotor Speed Above Self Excited Region

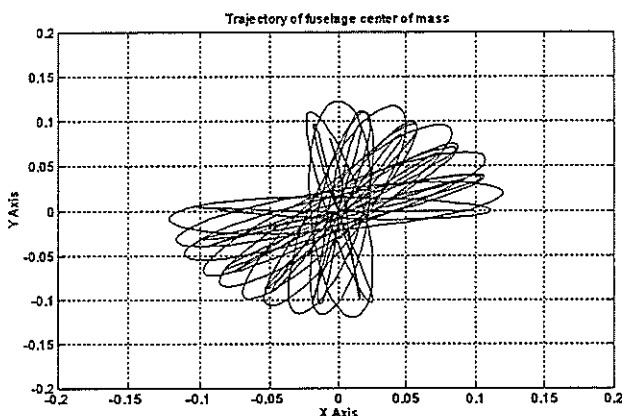


Figure 12.6 Fuselage Center of Mass Trajectory, Rotor Speed Above Self Excited Region

Figure 12.7 is the Coleman stability plot [Ref. 1] for the basic configuration. The solid lines indicate the boundaries of the self excited region and the dashed line marks the center of the self excited region. The X's indicate the operating points for the three cases shown in Figures 12.1 through 12.6.

In addition, a comparison was made between the simulation model and a time history solution of Coleman's and Feingold's equations. Bramwell [Ref. 4] derives Coleman's and Feingold's equation in a form equivalent to that of the simulation model with the blade displacements expressed in the rotating coordinate system and the fuselage displacements expressed in the fixed coordinate system. These equations were solved in the fixed coordinate system using an eigenvalue analysis and the solutions transformed back to rotating coordinate system. A comparison was

then made with the lead-lag displacement time history of the simulation model.

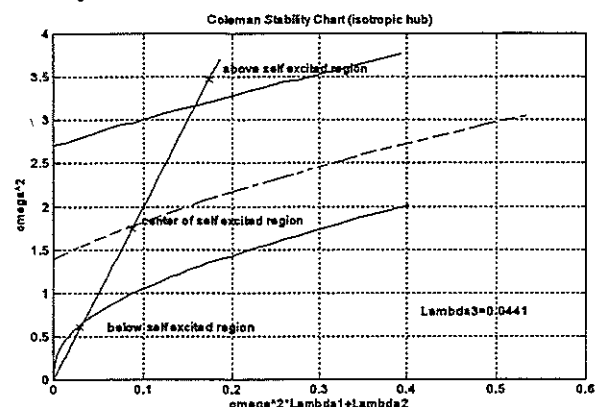


Figure 12.7 Coleman Stability Plot for Basic Case

Figure 12.8 shows the result of the comparison using the parameters of the basic configuration with a moderate amount of damping added to rotor blades and fuselage. Figure 12.8 shows excellent agreement between the two solutions with a departure between the two occurring only when displacements get very large. Thus, for the limiting case of an isotropic hub with linear spring stiffness and damping, the above comparison offers some amount of verification as to the accuracy of the simulation model.

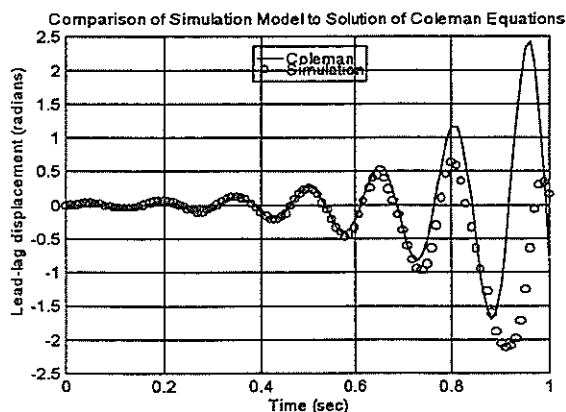


Figure 12.8 Comparison of Simulation Model to Coleman's Model

IV. EXAMPLE CASES

Moving on from the basic results and model verification, some of the more interesting cases that were simulated will now be discussed. Figure 12.9 shows a comparison between a case where all blade lead-lag dampers are

operating and a case where one damper is inoperative. The first plot of Figure 12.9 shows a rotor with all blade dampers operating, in the second plot, the blade associated with the bubble-line time history has its damper disabled by reducing the damping coefficient by two-thirds. As is evident from the plot, the stable case with full damper operation is made highly unstable by failing one damper.

Figure 12.10 shows the results of simulating damage to a rotor blade by reducing the mass of the bubble-line blade by 20%. The undamaged blades are forced to oscillate around a non-zero displacement position in order to compensate for the damaged blade, but the amplitudes of all the blade oscillations appear to be constrained.

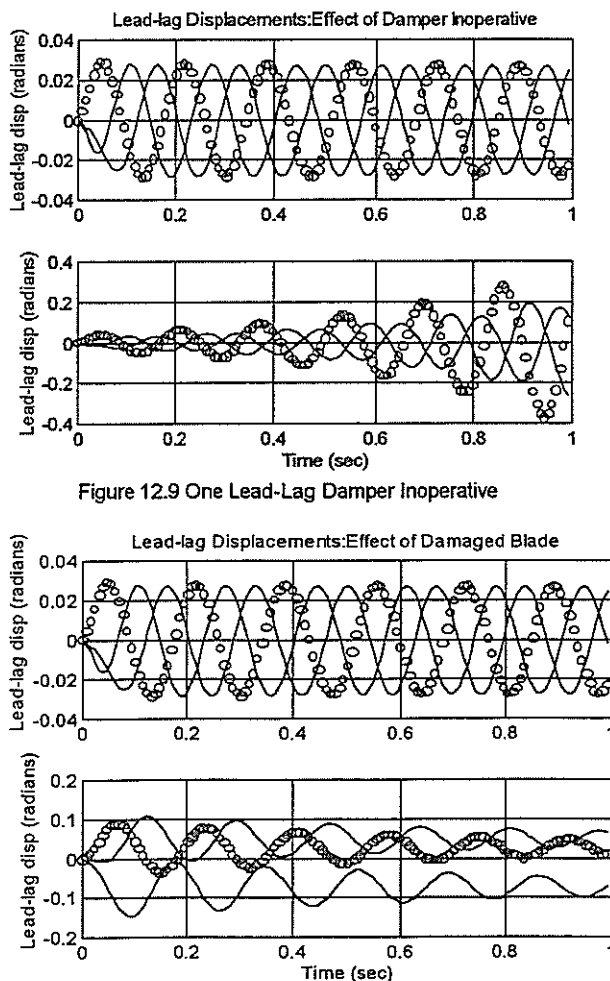


Figure 12.9 One Lead-Lag Damper Inoperative

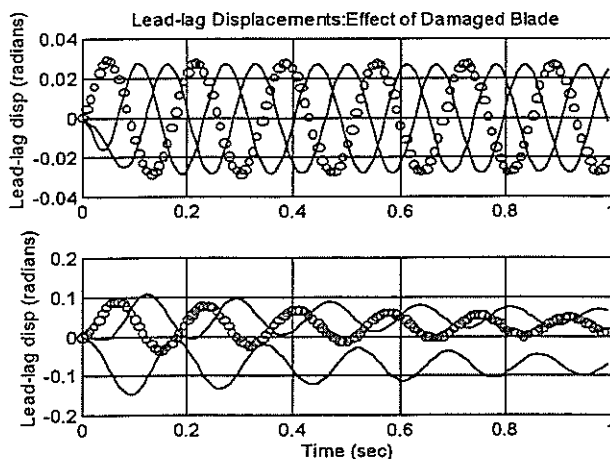


Figure 12.10 Simulated One Rotor Blade Damaged

Figure 12.11 shows the effect of introducing lead-lag stops in the model. The figure compares the time history of a blade with no

stops with that of a blade with spring stops positioned at ± 15 degrees (0.262 radians).

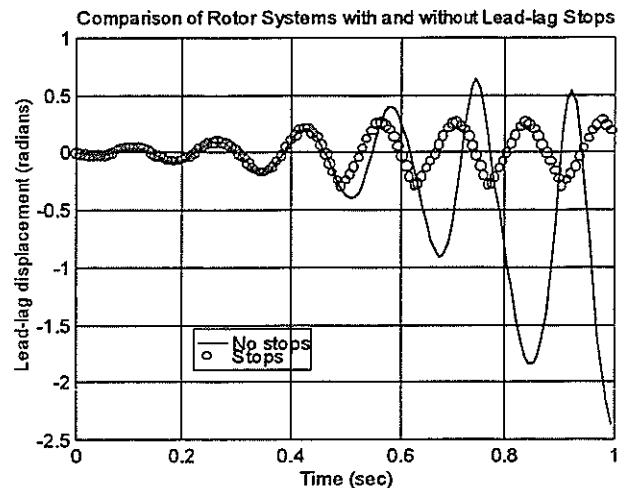


Figure 12.11 Effect of Lead-Lag Stops

The objective of the next set of simulations was to examine the effect of a nonlinear flexbeam incorporated into a bearingless rotor design. The nonlinear behavior of the flexbeam was assumed to be that of a Duffing spring where the restoring moment is given by

$$(M_{\zeta})_{Duffing} = K_e \zeta + K_d \zeta^3 \quad (7)$$

K_e is the linear stiffness and K_d the nonlinear stiffness. Simulations were conducted for several values of the nonlinear spring constant keeping the linear coefficient constant at 22,000 ft-lbs/radian. Results are shown in Figure 12.13. The primary effect of increasing the nonlinear spring constant is in limiting the amplitude of the lead-lag response. As shown in Figure 12.13, the case for $K_d = 0$ is very unstable and a helicopter caught in ground resonance in such a configuration would experience rapid catastrophic failure. By adding the hardening (cubic) term, the unbounded growth in amplitude can be checked, as is apparent from the response for the case of $K_d = 80,000$ ft-lbs/radian. As the amplitude increases, the magnitude of the nonlinear term becomes more influential and effectively changes the frequency of oscillation, shifting it outside of the unstable region and allowing the oscillations to decay. Once the amplitude decays to where the influence of the nonlinear term becomes small, the cycle repeats itself. While the limiting amplitudes for the nonlinear case of Figure

12.13 are still large for lead-lag displacements (on the order of 15 to 20 degrees), this limiting behavior may be enough to prevent destruction of an aircraft if ground resonance were excited. In flight, when lead-lag displacements are small, the hardening effect of a nonlinear flexbeam would be negligible, and could be designed to act as soft-in-plane in order to minimize hub moments.

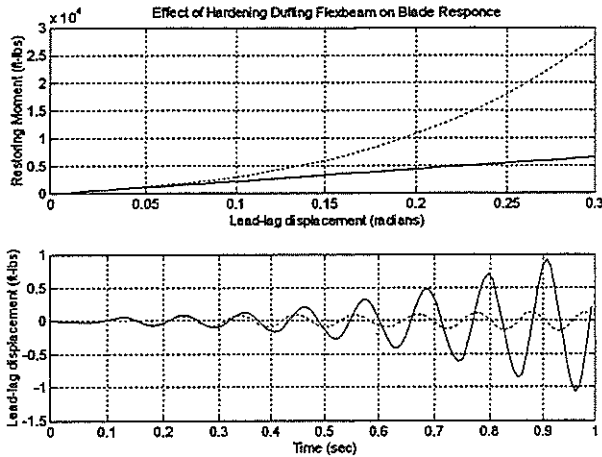


Figure 12.13 Effect of Hardening Duffing Flexbeam on Lead-lag Response

It is important to note that the elastic behaviors of the flexbeams modeled by the curves in the upper plot of Figure 12.13 are purely hypothetical and were selected arbitrarily in order to illustrate the effect that nonlinear elastic behavior could have on rotor system response and stability.

V. ACTIVE ROTOR CONTROL AND THE MOVING BLOCK TECHNIQUE

One of the drawbacks of performing direct numerical simulation of dynamic systems is that time histories of system degrees of freedom only offer qualitative information on the effect that certain system parameters have on system stability or performance. In order to quantify the effects of varying certain system parameters, such as rotor speed, flex-beam stiffness, and active control inputs, on rotor-fuselage stability in the ground resonance regime, a method was needed to determine system damping levels from the system time histories. Moving Block Analysis, a technique first applied at Lockheed in the 1970's, is a discrete method of analyzing a transient time history to obtain modal damping and frequency. The technique is described in

some detail by Hammond and Dogget [Ref. 5] and Bousmann and Winkler [Ref. 6].

A MATLAB® based program was developed to apply the moving block technique to time history traces generated from coupled rotor fuselage simulations completed with the computational tool. For a sampled signal (in this case, the time trace resulting from a simulation) the Moving Block method is applied by first estimating the frequency of interest embedded in the signal using a Fast Fourier Transform (FFT). A block length is selected consisting of N_b data points. The magnitude of the Discrete Fourier Transform (DFT) of this block is then calculated. The block is then shifted one time step, and the DFT magnitude is calculated again. This process is repeated until the time block is at the end of the signal. The log of the magnitude of the DFT of each block is plotted against the start times of each block. The negative of the slope of the least squares fit of this plot divided by the damped frequency of the mode being measured yields the damping ratio.

The Moving Block program was used to quantify the effect of active rotor control on ground resonance. A simple fixed gain controller, similar to that used by Weller [Ref. 7], was incorporated into the more complicated simulation model (the model which adds rotor blade flap, fuselage pitch and roll, and aerodynamics to the simple rotor-fuselage model) using the following relationship which transforms fuselage pitch and roll into lateral and longitudinal swashplate inputs.

$$\begin{bmatrix} \theta_c \\ \theta_s \end{bmatrix} = \begin{bmatrix} K \cos(\phi) & K \sin(\phi) \\ -K \sin(\phi) & K \cos(\phi) \end{bmatrix} \begin{bmatrix} r_1 \\ r_2 \end{bmatrix} \quad (8)$$

Here, θ_c and θ_s are longitudinal and lateral cyclic blade pitch inputs respectively, r_1 and r_2 are fuselage roll and pitch, K is the feedback gain, and ϕ is the controller phase angle. For this study, stability measurements were made based on time histories of the orthogonal components of the rotor center of gravity offset. These time histories contain both the regressing and progressing mode contributions. The damping levels of these modes for various gain and phase settings were determined using the Moving Block program.

Figure 12.14 shows the rotor center of gravity offset response to a lead-lag perturbation for a baseline case where the

feedback gain, K , is set to zero. The high frequency component present in the initial part of the simulation is the progressing lead-lag mode and damps out quite quickly. The dominant low frequency trace is the regressing mode and is unstable for this case. Figure 12.15 shows the results of analyzing the time trace in figure 12.14 with the Moving Block analysis.

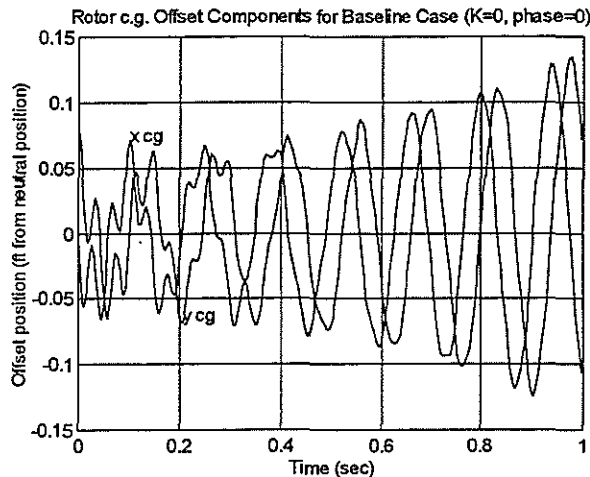


Figure 12.14 Rotor c.g. Offset Components for Baseline Case ($K=0$, $\phi=0$)

The upper plot of Figure 12.15 is the initial spectral analysis of the time trace computed using a FFT. The second plot refines the resolution of the FFT about the frequencies of interest. The third part of Figure 12.15 shows the plot of the moving block functions (see Ref. 4 and Ref. 5) for the regressing and progressing lead-lag modes with the straight line least square fits superimposed over them.

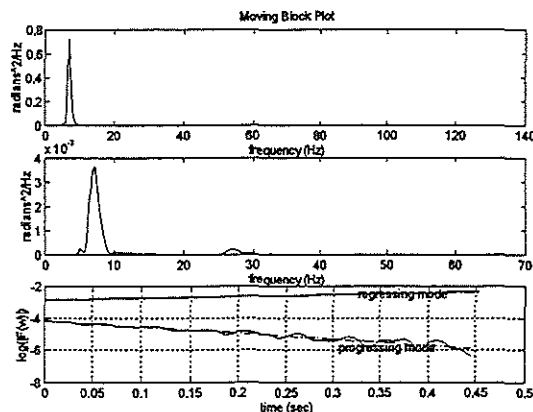


Figure 12.15 Results of Moving Block Analysis on Baseline Simulation ($K=0$, $\phi=0$)

Next, simulations were completed for controller phase sweeps at two different gain

settings and the regressing mode damping ratio was determined for each simulation using the Moving Block code. Figure 12.16 shows the results of combining the simulation model with the Moving Block code. For the gain settings tested, the controller does not stabilize the regressing mode, but this example illustrates the versatility of the modeling method and the engineering and design information that can be obtained from marrying the this computational tool with a system identification technique like Moving Block.

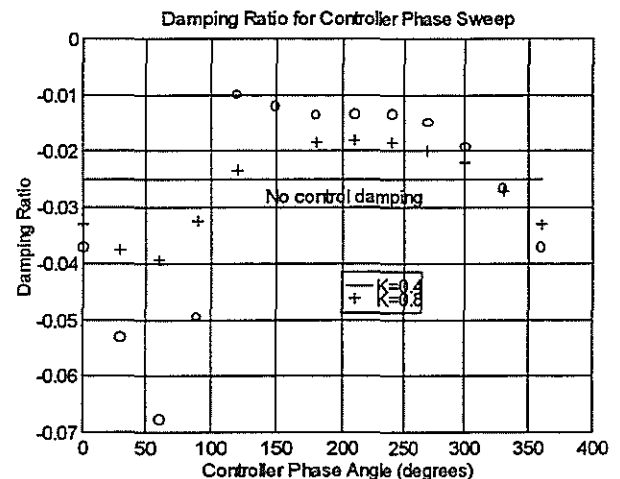


Figure 12.16 Damping Ratio For Controller Phase Sweep ($K=0.4$ and $K=0.8$)

VI. CONCLUDING REMARKS

A method for formulating and automatically coding the equations of motion of a coupled rotor-fuselage system by use of symbolic processing software and dynamic simulation software has been developed. The resulting mathematical models were used to perform simulations of coupled rotor-fuselage systems in ground resonance. Analysis of the dynamic and stability characteristics were quantified using the moving block technique. A simple rotor model was used to demonstrate essential characteristics of air/ground resonance and the effects that parameter variations such as rotor speed, flexbeam elastic behavior, damper failure, and rotor blade damage have on those characteristics. A more complex model, adding fuselage pitch and roll, rotor blade flap degrees of freedom, and aerodynamics, was then applied to demonstrate how the modeling technique could be used to explore the effect of active rotor control on ground resonance. The modeling technique proved to be a very

powerful tool in that it eliminated the time consuming process of manually deriving and coding the very complex equations of motion of a multi-degree of freedom rotor system into a dynamic simulation environment. By integrating SIMULINK® into the process, with its versatility in analyzing dynamic systems, the technique has direct application to the design of advanced technology rotor systems.

To summarize, among the features of the new modeling method are the following:

- All terms are included in the equations of motion at each time step of the simulation.
- All restrictions with respect to small angles and small displacements have been eliminated.
- No ordering schemes were used, in which case, a pre-selection process is generally carried out to determine which terms would be retained. Here, this is not required.
- Inherent highly reliable software, since manual coding of equations of motion has been eliminated.
- SIMULINK, as the simulation component of the method, provides a generic control/simulation environment that offers in itself a broad range of analysis capability for exploring air/ground resonance characteristics of both linear and non-linear rotor systems with or without active control.

VII. REFERENCES

1. Coleman, R. P., and Feingold, A. M., "Theory of Self Excited Mechanical Oscillations of Helicopter Rotors with Hinged Blades," NACA Report 1351, 1958.
2. Robinson, C. S., "Modeling and Analysis of Helicopter Ground Resonance Utilizing Symbolic Processing and Dynamic Simulation Software," Aeronautical Engineer's Thesis, Naval Postgraduate School, March 1997.
3. SIMULINK® *Dynamic Simulation Software User's Guide*, The MathWorks, Inc., 1992.
4. Bramwell, A. R. S., *Helicopter Dynamics*, Edward Arnold Publishers Ltd., London, 1976.
5. Hammond, C. E., and Doggett, R. V., "Determination of Subcritical Damping by Moving-Block/Randomdec Applications," *NASA Symposium on Flutter Testing Techniques*, NASA SP-415, Oct. 1975.
6. Bousman, W. G, and Winkler, D. J., "Application of the Moving Block Technique", *Proceedings of the 22nd Annual AIAA Structural Dynamics and Materials Conference*, 81-0653CP, April 1981.
7. Weller, W. H., "Fuselage State Feedback for Aeromechanical Stability Augmentation of a Bearingless Main Rotor," *Journal of the American Helicopter Society*, April 1996, pp. 85-93.